

Feedbacks between vegetation restoration and local precipitation over the Loess Plateau in China

Baoqing ZHANG¹, Lei TIAN^{1,2}, Xining ZHAO^{3*} & Pute WU³¹ Key Laboratory of Western China's Environmental Systems (Ministry of Education), College of Earth and Environmental Sciences, Lanzhou University, Lanzhou 730000, China;² Institute of Green Development for the Yellow River Drainage Basin, Lanzhou University, Lanzhou 730000, China;³ Institute of Soil and Water Conservation, Northwest A&F University, Yangling 712100, China

Received October 12, 2020; revised January 29, 2021; accepted March 2, 2021; published online May 6, 2021

Abstract The implementation of large-scale vegetation restoration over the Chinese Loess Plateau has achieved clear improvements in vegetation fraction, as evidenced by large areas of slopes and plains being restored to grassland or forest. However, such large-scale vegetation restoration has altered land-atmosphere exchanges of water and energy, as the land surface characteristics have changed. These variations could affect regional climate, especially local precipitation. Quantitatively evaluating this feedback is an important scientific question in hydrometeorology. This study constructs a coupled land-atmosphere model incorporating vegetation dynamics, and analyzes the spatio-temporal changes of different land use types and land surface parameters over the Loess Plateau. By considering the impacts of vegetation restoration on the water-energy cycle and on land-atmosphere interactions, we quantified the feedback effect of vegetation restoration on local precipitation across the Loess Plateau, and discussed the important underlying processes. To achieve a quantitative evaluation, we designed two simulation experiments, comprising a real scenario with vegetation restoration and a hypothetical scenario without vegetation restoration. These enabled a comparison and analysis of the net impact of vegetation restoration on local precipitation. The results show that vegetation restoration had a positive effect on local precipitation over the Loess Plateau. Observations show that precipitation on the Loess Plateau increased significantly, at a rate of 7.84 mm yr^{-2} , from 2000 to 2015. The simulations show that the contribution of large-scale vegetation restoration to the precipitation increase was about 37.4%, while external atmospheric circulation changes beyond the Loess Plateau contributed the other 62.6%. The average annual precipitation under the vegetation restoration scenario over the Loess Plateau was 12.4% higher than that under the scenario without vegetation restoration. The above research results have important theoretical and practical significance for the ecological protection and optimal development of the Loess Plateau, as well as the sustainable management of vegetation restoration.

Keywords Coupled land-atmosphere modeling, Vegetation restoration, Water balance, Hydrometeorology, Ecohydrology

Citation: Zhang B, Tian L, Zhao X, Wu P. 2021. Feedbacks between vegetation restoration and local precipitation over the Loess Plateau in China. *Science China Earth Sciences*, 64(6): 920–931, <https://doi.org/10.1007/s11430-020-9751-8>

1. Introduction

The Chinese government has implemented the Grain for Green Project since 1999, aimed at improving the vegetation fraction of the Loess Plateau and controlling soil erosion.

Over the past two decades since the start of the project, a large area of sloping farmland has been returned to grassland or forest. The vegetation restoration has had significant impacts (Zhang et al., 2011), and the sediment yield of the Yellow River Basin has been greatly reduced (Wang et al., 2006; Hu et al., 2008; Chen et al., 2015; Yang D W et al., 2015; Wang et al., 2016; Zhang et al., 2016). Large-scale

* Corresponding author (email: zxn@nwsuaf.edu.cn)

vegetation restoration will affect the water-energy balance between the atmosphere and land surface by changing the underlying surface conditions, causing changes in water and energy factors such as evapotranspiration, soil infiltration, surface runoff, net radiation, sensible heat and latent heat flux. In turn, these changes will influence the strengths of interactions between the land surface and atmosphere, which will feed back into regional climate and local precipitation process (Yang D W et al., 2015; Tang, 2020). Therefore, in the context of modern conditions, and in order to ensure sustainable and optimal development of vegetation, how to quantitatively analyze the feedback effects of vegetation restoration on regional climate and local precipitation in the Loess Plateau has become an urgent scientific problem (Wang et al., 2011; Su and Fu, 2013; Feng et al., 2016).

Exploring the direction of changing land use trends on the Loess Plateau, assessing the degree of improvement in vegetation fraction, and analyzing the temporal and spatial trends of key vegetation and surface parameters that affect surface water balance, together form the basis for quantitative assessment of the regional climate effects caused by large-scale vegetation restoration. Vegetation restoration on the Loess Plateau mainly requires measures such as returning farmland to forests (or grassland), closing hills for afforestation (or grassland), and afforestation (or grassing over) of barren hillsides. The direct impacts of these measures are reflected in three aspects: (1) changes in land-use type; (2) changes of key vegetation parameters that affect the land-surface water balance, such as leaf area index (*LAI*), vegetation fraction; and (3) changes in key land surface parameters that affect the energy balance through changes in albedo (Ren et al., 2014; Liang et al., 2015). At present, research on the regional hydrological effects of large-scale vegetation restoration mainly uses remote sensing inversion techniques to obtain parameters such as land use type, *LAI*, vegetation fraction and land surface albedo, and to analyze their temporal and spatial variation trends. These parameters are then used to drive land surface models or distributed hydrological models in offline simulations, which in turn are analyzed to explore the influence of vegetation restoration. However, existing studies often ignore the feedback effect of land surface processes on regional climate, and research on the effects of changes in vegetation and land surface parameters on land-atmosphere interaction and local precipitation is somewhat lacking (Xiao et al., 2008; Ren et al., 2014).

Chen et al. (2015), Liang et al. (2015), Wang et al. (2016), Feng et al. (2016) and Zhang et al. (2016) have shown that, since the beginning of the 21st century, vegetation on the Loess Plateau has become greener and the land cover has increased significantly. However, significant surface water changes have also occurred during the vegetation restoration, which are mainly reflected by a rapid increase in water consumption through evapotranspiration on the Loess Pla-

teau, and a sharp decrease in the runoff coefficient. As a result, runoff of the Yellow River Basin has dropped sharply, and the deficit between the supply and demand for regional water resources has further intensified. The intensity of vegetation restoration in some areas has reached the upper limit of the area's capacity for vegetation, which means that if the intensity of vegetation regeneration is further increased, new ecological problems such as soil desiccation, vegetation degradation and excessive water consumption will occur (Wang et al., 2018; Yang et al., 2018). In addition to the above-mentioned impacts on the land-surface water budget, large-scale vegetation restoration on the Loess Plateau will have a feedback effect on the regional climate (by changing the relationship between the surface water-energy balance and the atmosphere) by affecting the exchange of materials and energy between the land and atmosphere. Changes in regional climate will further affect the distribution of land surface water and energy, cause changes in the intensity of land-atmosphere interaction, and could even have additional effects on hydrological processes such as local precipitation, evapotranspiration, vegetation interception, and soil infiltration (Gibbard et al., 2005; Liu et al., 2011; Wen et al., 2012; Wu and Zhang, 2013; Hirsch et al., 2014; Hu et al., 2015). This again highlights why evaluating the feedback effect of large-scale vegetation restoration on local precipitation, on the basis of changes in the intensity of land-atmosphere interactions, is an important scientific issue that urgently needs to be studied.

Coupled land-atmosphere models can improve the ability of land surface models to simulate surface processes, while providing a more accurate underlying surface boundary for atmospheric processes, thereby effectively linking high-resolution regional climate models with land surface models. Coupled land-atmosphere models especially consider the feedback effect of land surface processes on regional climate, and can improve the accuracy of regional climate models to a certain degree. The Weather Research and Forecasting Model (WRF) is a mesoscale regional climate model developed by the National Center for Atmospheric Research (NCAR), and implements the latest research developments in mesoscale climate simulation (Wang and Sun, 2013). The WRF model can be bidirectionally coupled with different land surface process models (Jin and Wen, 2012), including Noah (Chen et al., 1996), and can be used to quantitatively analyze the impact of vegetation dynamics on regional climate and local precipitation feedback effects (Subin et al., 2011; Xiong et al., 2014; Wang et al., 2015; Yang Y et al., 2015). WRF uses MODIS land-use data by default. However, the default MODIS land-use data were acquired around the year 2000. For the Loess Plateau, where large-scale vegetation restoration has been carried out, the default MODIS land-use data in WRF can only reflect the land-use types before vegetation restoration in this region;

therefore, its timeliness is clearly suboptimal. The time range of dynamic land use data provided by the European Space Agency Climate Change Initiative (ESA CCI) is from 1992 to 2019. It is dynamically updated every year and can accurately reflect the changes in land-use types after large-scale vegetation restoration (Ganguly et al., 2010). In addition, since the current version of the WRF-Noah coupling model simplifies biogeophysical processes, its *LAI*, vegetation fraction and albedo are estimated based on the land-use type combined with a parameter comparison table. This means that once the land use type is determined, the corresponding vegetation and surface parameters remain fixed. Without considering the real dynamic changes of land-use types and vegetation fraction, the model cannot realistically reflect the conditions and dynamic changes of vegetation and surface parameters following large-scale vegetation restoration on the Loess Plateau.

Given the above limitations, it is necessary to couple the land surface process model to the regional climate model. Based on the dynamic land-use data, dynamic vegetation and ground surface parameters obtained from remote sensing, a two-way land-atmosphere coupled model considering the vegetation dynamic changes is constructed. According to the two-way land-atmosphere coupled model, the impacts of vegetation fraction changes on regional climate and land surface processes are discussed, which is of great benefit in managing vegetation restoration of the Loess Plateau and the rational use of limited water resources (Luo et al., 2013; Hu et al., 2015). The regional climate and land-use patterns of the Loess Plateau have together undergone dramatic changes, so dynamic land-use data must be used as the input in the WRF-Noah coupled model, and combined with dynamic *LAI*, vegetation fraction and albedo, to improve the simulation of vegetation and surface parameters following vegetation restoration. Furthermore, by considering the impacts of large-scale vegetation restoration on the water cycle and land-atmosphere interaction of the basin, the regional hydrological effects of large-scale vegetation restoration can be accurately described, and the response of local precipitation to vegetation restoration on the Loess Plateau can be quantitatively evaluated. The results can provide scientific support for ecological protection and optimal development of the Loess Plateau.

2. Study area

The Loess Plateau is located in the upper and middle reaches of the Yellow River (33°43′–41°16′N, 100°54′–114°33′E), and includes the western Taihang Mountains, eastern Wushaoling and northern Qinling, and lies south of the Great Wall. This region is located on the edge of the warm temperate monsoon climate zone, and is mainly characterized by

a continental climate and monsoon instability. The average annual precipitation increases from northwest to southeast (150–820 mm). The region has four distinct seasons, and the annual average temperature is 3.6–14.3°C. The altitude range is 1000–1500 m, and the total area is about 64×10^4 km². The Loess Plateau has suffered from a long-term lack of vegetation protection, the ecological environment is fragile, and the soil is poorly consolidated. Intense rainstorms have caused serious soil erosion in this area. To improve the vegetation fraction of the Loess Plateau and control soil erosion, the Chinese government has invested considerable labour, material and financial resources in the area. Especially since 1999, large-scale vegetation restoration measures such as returning farmland to forest (or grassland), closing hills to reforestation (or grassland) and afforestation (grassing over) of barren hills has been implemented. The vegetation types of the Loess Plateau, in order from southeast to northwest, comprise forest steppe, typical steppe, desert steppe and desert. The vegetation fraction is consistent with the precipitation pattern, and gradually improves from northwest to southeast.

3. Materials and methods

The coupled land-atmosphere model used in this study is WRF-Noah (V3.6.1), where WRF is a state-of-the-art Mesoscale Weather Forecast Model, and Noah is a land surface process scheme in WRF. This model is mainly used for research on regional climate change and land-atmosphere interaction (Emmanouil et al., 2021; Gao et al., 2020). In this study, the center of the WRF simulation domain is at 37°N, 108°E. The projection method is the Lambert Equiangular Conic Projection, suitable for mid-latitude regions, and the two standard latitudes are 30°N and 60°N. The forcing data for the WRF-Noah model are the ERA-Interim reanalysis data from the European Centre for Medium-Range Weather Forecasts (ECMWF) (Hersbach and Dee, 2016). The temporal resolution of ERA-Interim data is 6 h, the horizontal resolution is $0.5^\circ \times 0.5^\circ$, and the vertical layering has 27 layers. The horizontal resolution of the WRF-Noah model is 10 km. The dataset used to verify the simulation results is the China Meteorological Forcing Dataset (CMFD) (Yang et al., 2010; He et al., 2020). The CMFD dataset contains variables such as precipitation and near-surface temperature from 2000 to 2015, and its temporal and spatial resolutions are 3 h and $0.1^\circ \times 0.1^\circ$, respectively. CMFD incorporates observation data from 740 national stations in China, and a number of studies have verified the accuracy and reliability of the dataset (Chen et al., 2011; Yang et al., 2017). Since the horizontal resolution of CMFD (0.1°) is very similar to the WRF-Noah model (10 km), no interpolation was performed in the verification

of the WRF-Noah simulation.

This study designed two sets of simulation experiments, both of which used ERA-Interim reanalysis data and adopted the same combination of parameterization schemes. The first set of experiments was the control experiment (WRF CTL), which assumed that no vegetation restoration has been carried out and the land cover of the Loess Plateau remained in the state prior to vegetation restoration. WRF CTL uses the default static land-use data, static vegetation and surface characteristic parameters to drive the WRF-Noah model and simulate precipitation in the study area from 2000 to 2015. This experiment represents a hypothetical scenario where no large-scale vegetation restoration has occurred. The second set of experiments (WRF DYN) used dynamic land use, dynamic vegetation, and surface parameters obtained from remote sensing data to drive the WRF-Noah model and simulate precipitation during the same period as that of WRF CTL. This experiment represents a real scenario of large-scale vegetation restoration. Based on the two simulations, we can explore in detail the feedback mechanisms in regional climate and local precipitation associated with large-scale vegetation restoration over the Loess Plateau.

Dynamic vegetation data were converted to land surface data from 2000 to 2015, in a format that can be recognized by the WRF-Noah model. The vegetation and land surface data sources were the Global Land Surface Satellite (GLASS) (Xiao et al., 2016) dataset and the ESA CCI land cover dataset (ESA, 2017); both are based on remote sensing. Dynamic vegetation data comprise land-use type, *LAI*, vegetation fraction and land surface albedo (see Table 1 for details). We have reclassified and resampled these remote sensing data products. The nearest neighbor interpolation method was used for the interpolation of land-use type data, and bilinear interpolation was used for other data. Finally, the key vegetation and land surface parameters needed for the WRF-Noah model were obtained, including land use type (*LU_INDEX*), land use type area ratio (*LANDUSEF*), land water mark (*LANDMASK*), vegetation fraction (*GREENFRAC*), leaf area index (*LAI*), land surface albedo (*ALBEDO*) (the variable names in the WRF-Noah model are in parentheses). Quantitative assessments of the trends of all variables in this study are based on the Theil-Sen Slope (Theil, 1950; Sen, 1968) trend analysis method.

4. Results

4.1 Analysis of temporal and spatial changes of vegetation fraction on the Loess Plateau

After the implementation of large-scale vegetation restoration, the land surface coverage of the Loess Plateau has improved significantly, and ecological restoration has achieved good results. The area of forest increased by 16.5%, the area of grassland increased by 7.6%, and the area of bare land and desert decreased by 29.0%. As shown in Figure 1, areas with a significant increasing trend in *LAI* account for 53% of the total area of the Loess Plateau. Here, the increasing trend of *LAI* was most obvious in the hilly gully region of the southeast Loess Plateau. The average rate of increase of *LAI* in the Loess Plateau was $1.22\% \text{ yr}^{-1}$, and the cumulative increase in *LAI* from 2000 to 2015 was 18.3%. In addition, the vegetation fraction has also shown a significant increasing trend, and the areas with a significant increase in vegetation fraction account for 73% of the total area in the Loess Plateau. The vegetation fraction also increased most significantly in the hilly gully region in the southeast of the study area. The average rate of increase in vegetation fraction on the Loess Plateau was $2.71\% \text{ yr}^{-1}$, and the cumulative increase in vegetation fraction from 2000 to 2015 was 40.7% (Figure 1). With the increase of *LAI* and vegetation fraction, the land surface albedo of the Loess Plateau has shown a significant decreasing trend, with an average decrease of $-0.50\% \text{ yr}^{-1}$, and a cumulative decrease of 7.5% from 2000 to 2015. Spatially, the area where the land surface albedo of the Loess Plateau decreased significantly accounts for 49% of the total area (Figure 1). The increase in vegetation fraction and the decrease in land surface albedo meant that more shortwave radiation was absorbed by the land surface. Moreover, the increase in CO_2 concentration led to an increase in long-wave radiation (Piao et al., 2019). As a result, the net absorbed radiation on the Loess Plateau increased significantly, and more energy was transferred into the regional climate and hydrological systems. This will have had a positive effect on surface temperature, air temperature, evapotranspiration and the vertical transport of water vapor; the intensity of water circulation in the basin will also have increased.

Table 1 Summary of various datasets used in this study

Dataset	Variable	Time period	Temporal resolution	Spatial resolution
ERA-Interim Reanalysis Dataset	Wind, specific humidity, temperature, etc., at different pressure levels	1999–2015	6 h	0.5°
ESA CCI Land Cover Dataset	Land use/land cover	1999–2015	Yearly	0.3 km
GLASS	<i>LAI</i> , vegetation fraction, and surface albedo	2000–2015	Daily	1 km
CMFD	Precipitation, and air temperature	2000–2015	3 h	0.1°

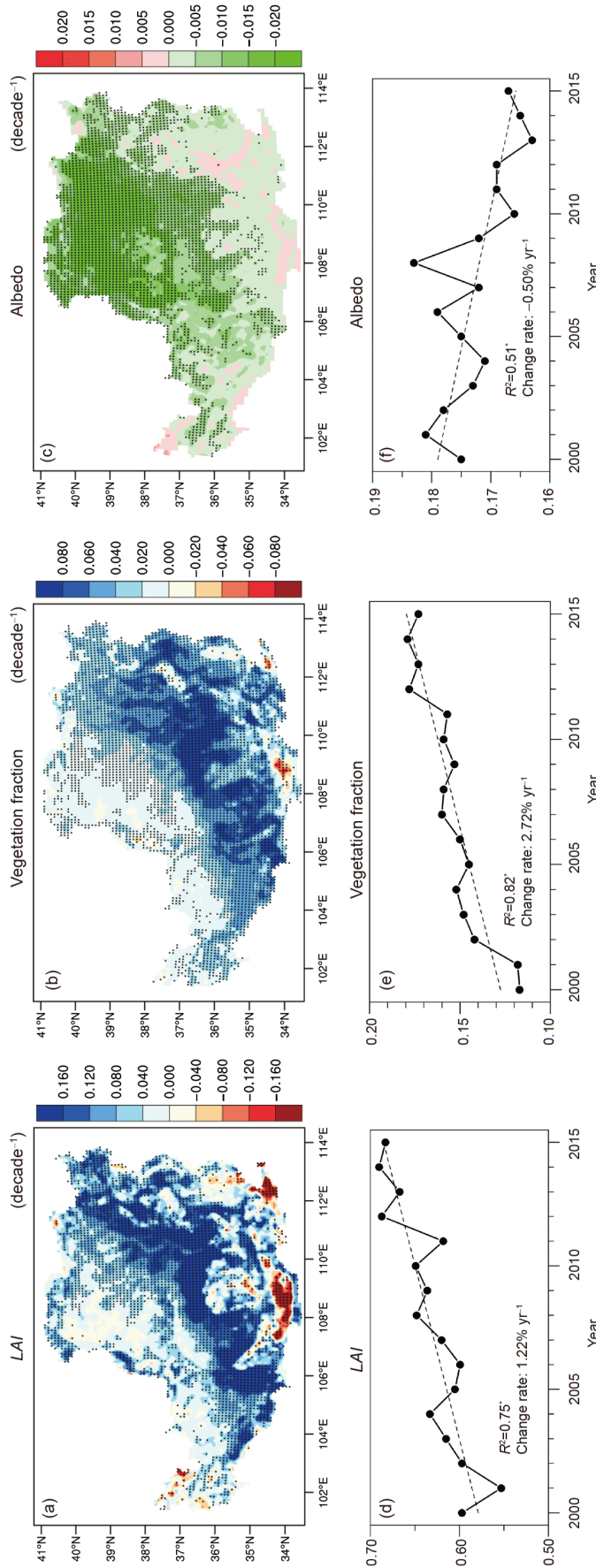


Figure 1 Spatiotemporal change of *LAI* ((a) and (d)), vegetation fraction ((b) and (e)), and albedo ((c) and (f)) in the Loess Plateau for the period 2000 to 2015. The dots in the top plots denote the statistical significance of the linear trend at the 95% confidence level. The dashed lines in the bottom plots denote linear trends in the time series. The rate of change (%) for each variable is also shown in the bottom plots, and the asterisk denotes the statistical significance of the linear trend at the 95% confidence level.

4.2 Accuracy assessment of the WRF-Noah precipitation simulation considering the vegetation dynamic changes

Determining the accuracy of a regional climate simulation is a prerequisite when using a coupled land-atmosphere model to effectively explore the feedback effect of vegetation restoration on the local precipitation in the Loess Plateau (Yu et al., 2010; Bao et al., 2015). This study conducted a systematic sensitivity test of the physical schemes, to provide an optimized WRF implementation for the regional climate simulation of the Loess Plateau, thereby improving the accuracy of precipitation simulation in this area. The simulation period of the sensitivity test was selected as July 2007, as the precipitation during this month was close to the multi-year climatic average precipitation in the study area. Each simulation period covered June and July in 2007, of which June was the spin-up period (excluded from the evaluation). The sensitivity tests considered three types of parameterization schemes closely related to the precipitation formation process: cloud microphysics schemes, planetary boundary layer schemes and cumulus convection schemes. Overall, we tested 11 cloud microphysical solutions, 8 atmospheric boundary layer solutions, and 7 cumulus convection solutions provided by the WRF model. Other physical schemes in the model remained unchanged, specifically including: the longwave radiation scheme of the Rapid Radiative Transfer Model (Mlawer et al., 1997), the shortwave radiation scheme of Dudhia (Dudhia, 1993) and the land surface process scheme of Noah (Chen et al., 1996).

Figure 2a shows the analysis results of the sensitivity test for the cloud microphysics scheme. The spatial correlation coefficients (PCC) of each experiment are concentrated at around 0.65, and the root mean square error (RMSE) varies from 1.05 to 1.32. Among them, CAM 5.1 (Neale and Hoskins, 2010) performed best (PCC maximum 0.66, RMSE 1.14). Generally speaking, the choice of cloud microphysical scheme has no obvious impact on precipitation simulation in

the study area. Based on the sensitivity test of the cloud microphysical parameterization scheme, the sensitivity test of the atmospheric boundary layer scheme was carried out; the results are shown in Figure 2b. The precipitation simulation in the study area was more sensitive to the atmospheric boundary layer scheme, and the PCC distribution range was 0.59–0.71. Among them, MYNN 2.5 (Nakanishi and Niino, 2006) achieved the highest PCC (0.71). Therefore, it is believed that the MYNN 2.5 scheme can better reflect the precipitation formation process in the study area. On the basis of the first two sensitivity experiments, the final test to select the scheme for cumulus convection parameterization was carried out, covering the 8 cumulus convection schemes. As shown in Figure 2c, precipitation simulation on the Loess Plateau is most sensitive to the cumulus convective parameterization schemes, and the results of the schemes are significantly different (PCC and RMSE are in the ranges of 0.56–0.72 and 0.88–1.18, respectively). The Kain-Fritsch (Kain, 2004) scheme performed best, with a higher PCC (0.71), and the degree of spatial variability was closer to the CMFD. Therefore, based on the three sets of sensitivity tests, this study compared and selected the optimal WRF parameterization scheme combination that most accurately reproduced the precipitation in the Loess Plateau. This combination comprised the RRTM longwave radiation scheme, Dudhia shortwave radiation scheme, CAM5.1 cloud microphysics scheme, MYNN2.5 atmospheric boundary layer scheme, Kain-Fritsch cumulus convection scheme and Noah land surface process scheme.

Although running WRF with the optimal parameterization scheme can greatly improve the accuracy of precipitation simulation on the Loess Plateau, the simulation results still have some errors (the total observed precipitation in July 2007 was 99 mm, and the simulated precipitation was 87 mm). One source of precipitation error arises because the experiments described above all use the WRF default static land surface data, which cannot effectively reflect the drastic land surface changes on the Loess Plateau after large-scale

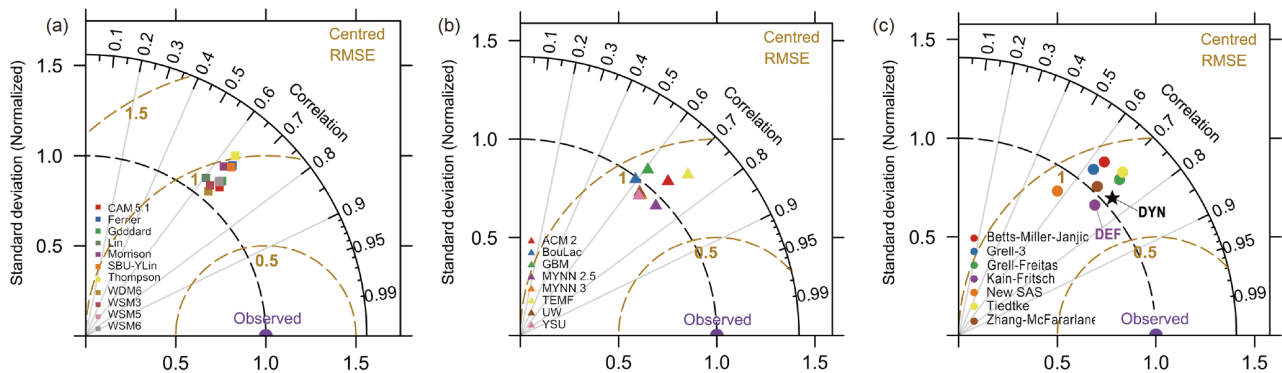


Figure 2 Comparison of sensitivity tests for different categories of the parameterization schemes in the WRF model. (a) Microphysics schemes; (b) planetary boundary layer schemes; (c) cumulus schemes. The pentagram in (c) denotes the precipitation simulated by WRF with dynamic vegetation, while the purple dot denotes the precipitation simulated by WRF without dynamic vegetation.

vegetation restoration. Therefore, this study also considers the optimized combination of schemes when using the 2007 land-cover data to drive the model, and explores the impact of vegetation dynamics on the precipitation simulation. As shown in Figure 2c, after considering the true surface changes, the WRF precipitation simulation was further improved (the PCC is 0.74), and the simulated total precipitation in July was 102 mm. In summary, the land-atmosphere coupling model WRF-Noah, which considers vegetation dynamics, can accurately reproduce the precipitation distribution on the Loess Plateau.

4.3 Quantitative assessment of the feedback effect of large-scale vegetation restoration on local precipitation

In this study, the dynamic changes of vegetation parameters (including land-use, vegetation fraction, *LAI*, and albedo) were coupled with the WRF model to construct a WRF-Noah two-way land-atmosphere coupled model that considers the vegetation dynamics. By comparing and analyzing the differences between the real scenario of vegetation restoration (WRF DYN) and the hypothetical scenario of no vegetation restoration (WRF CTL), it is found that the increase in evapotranspiration and water vapor flux caused by large-scale vegetation restoration have had a positive on local precipitation (Figure 3). This has been mediated through a series of changes in land-atmosphere interactions, triggered by vegetation restoration: increasing *LAI* and vegetation fraction, decreasing albedo, increasing net radiation, and increasing humidity and local water vapor flux. This is one of the main reasons that caused precipitation on the Loess Plateau to increase at a rate of 7.84 mm yr^{-2} (based on CMFD precipitation data) from 2000 to 2015. As shown in Figure 3, the simulation results of the WRF-Noah land-atmosphere coupling model based on the vegetation dynamic changes show that the average precipitation in the Loess Plateau region increased at a rate of 6.15 mm yr^{-2} under the real scenario of large-scale vegetation restoration. The correlation coefficient between simulated precipitation and ob-

served precipitation is 0.88, the RMSE is 69 mm yr^{-1} , and the absolute error is -14 mm yr^{-1} . In contrast to the WRF DYN scenario, the simulation results of the WRF-Noah land-atmosphere coupling model under the WRF CTL scenario show that if large-scale vegetation restoration had not been carried out, the average precipitation across the Loess Plateau would only have increased at a rate of 3.85 mm yr^{-2} . In this scenario, the correlation coefficient between simulated precipitation and observed precipitation is only 0.84, the RMSE is 101 mm yr^{-1} , and the absolute error is -70 mm yr^{-1} . The above results show that the simulation accuracy of WRF-Noah when including vegetation dynamics, is significantly better than that of WRF-Noah when not including vegetation dynamics. The above comparison also shows that large-scale vegetation restoration has affected the land-atmosphere interactions, resulting in an additional precipitation increase of 2.3 mm yr^{-2} (the difference between 6.15 and 3.85 mm yr^{-2}). The contribution of vegetation restoration (2.3 mm yr^{-2}) to the total precipitation increase on the Loess Plateau was about 37.4%, while the remaining 62.6% (3.85 mm yr^{-2}) was attributed to larger-scale changes in water vapor dynamics (Figure 3).

As shown in Figure 4, the annual precipitation on the Loess Plateau obtained from the two simulation experiments (WRF DYN and WRF CTL) showed a decreasing trend from southeast to northwest. The average regional precipitation in WRF DYN (443 mm yr^{-1}) was 12% higher than that in WRF CTL (388 mm yr^{-1}). The areas with the largest differences in precipitation between the two simulations were in the hilly gully region of the southeast Loess Plateau. In this area, the precipitation in WRF DYN was generally $>60 \text{ mm yr}^{-1}$ higher than that in WRF CTL, and in some areas the difference exceeded 100 mm yr^{-1} . This result is consistent with the trends in vegetation fraction, *LAI* and land surface albedo in the Loess Plateau (Figure 1) and indicates that the local precipitation pattern in the study area shows a significant positive response to large-scale vegetation restoration. Thus, vegetation restoration has a positive effect on annual precipitation in the Loess Plateau. In addition to the spatial differences in

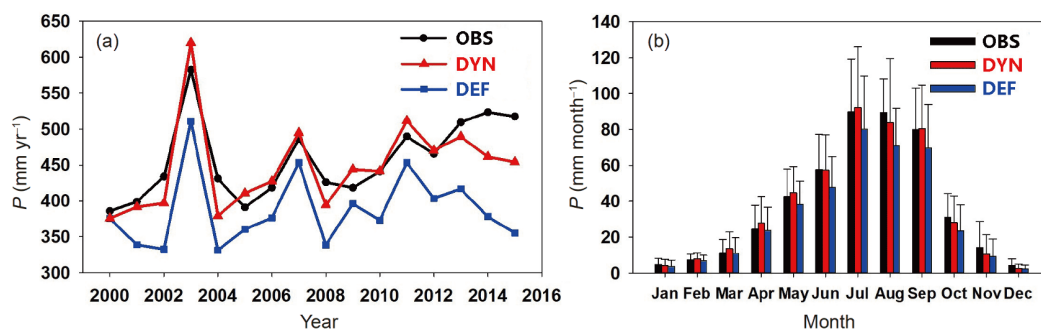


Figure 3 Comparison between WRF precipitation simulations (DYN and DEF) and CMFD observation (OBS). (a) Inter-annual variations; (b) intra-annual variations. The red line and bar represent WRF simulated precipitation with the dynamic vegetation scenario (DYN), the blue line and bar represent that with the default vegetation scenario (DEF). Meanwhile, the black line and bar represent the CMFD observations.

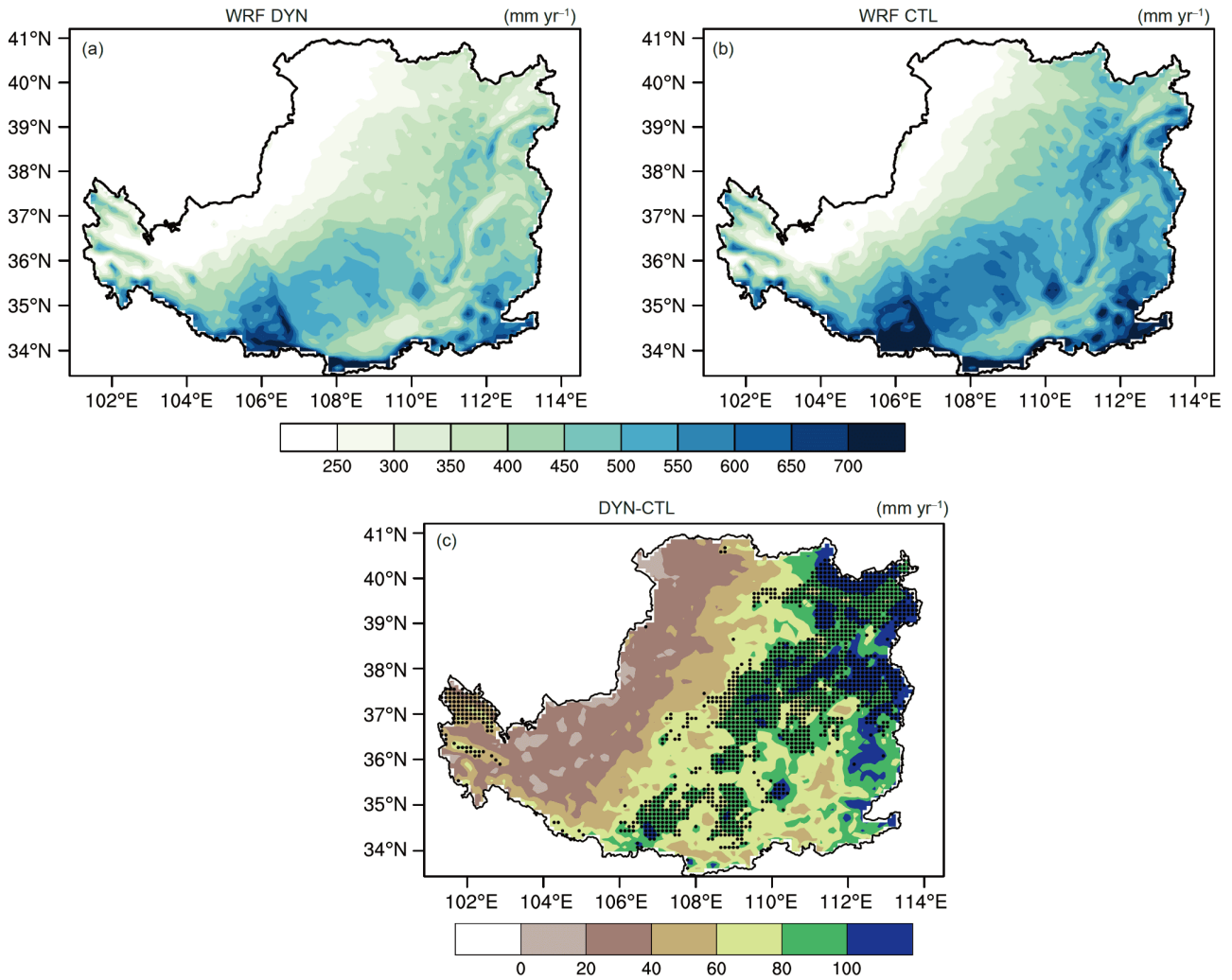


Figure 4 The climatology (2000–2015) of annual precipitation (mm yr^{-1}) in the two WRF precipitation simulations. (a) DYN and (b) CTL. The difference (DYN minus CTL) of annual precipitation climatology between DYN and CTL is shown in (c), and the dots in plot (c) denote statistical significance at the 95% confidence level.

annual precipitation, there were also significant spatial differences across the Loess Plateau in the annual precipitation trends obtained from WRF DYN and WRF CTL. The average trend in precipitation in WRF DYN was 35% higher than that in WRF CTL, and the areas with increasing precipitation trends were also mainly distributed in the hilly gully region of the southeast Loess Plateau (Figure 5).

4.4 Analysis of feedbacks between vegetation dynamics and regional climate

The above simulation results show that large-scale vegetation restoration on the Loess Plateau can increase local precipitation to a certain extent. To better clarify the feedbacks between vegetation dynamics and regional climate, this study analyzed the changes in the transfer and exchange of water vapor, energy, and momentum under large-scale vegetation restoration from the perspectives of the hydro-

logical and thermodynamic characteristics of the underlying surface changes, atmospheric boundary layer development, and atmospheric dynamics. As shown in Figure 6, we comprehensively analyzed and compared the physical quantities output by both WRF-Noah simulations (under the dynamic vegetation and static vegetation scenarios) during the period from 2000 to 2015. It can be seen that the vegetation fraction and *LAI* under the dynamic vegetation scenario were significantly higher than those under the no vegetation restoration scenario (increases of +9.02% and +13.42%, respectively). On the one hand, the increase in vegetation fraction led to a decrease in regional albedo (−5.11%), thereby increasing the shortwave radiation received, which can be understood as the land-surface heating effect of the vegetation restoration. On the other hand, an increase in vegetation led to greater evapotranspiration (+17.18%) and latent heat flux (+4.11 W m^{-2}), which had a cooling effect on the land surface. However, the heating effect was greater

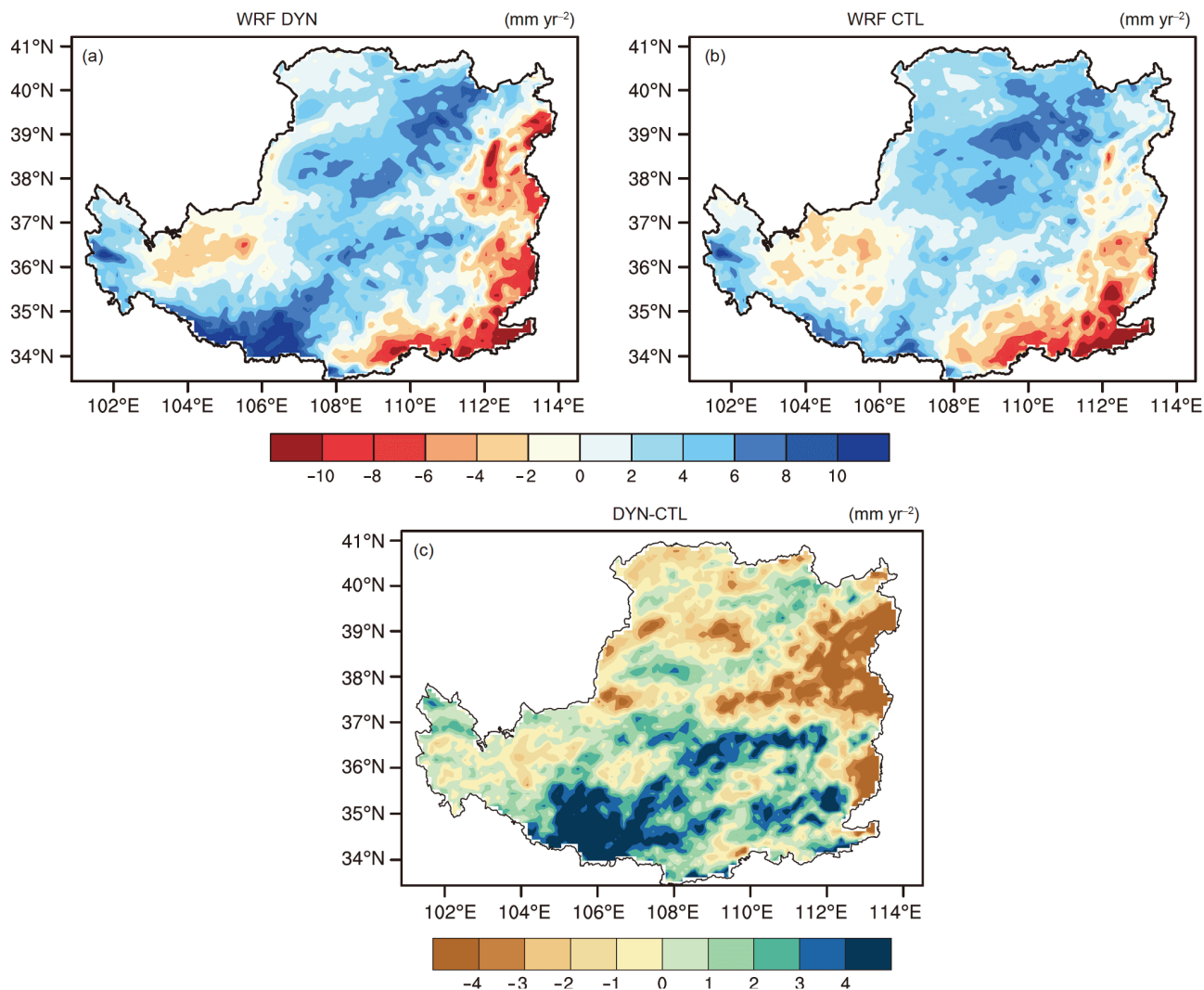


Figure 5 Spatial patterns of the linear trend (mm yr^{-2}) in WRF simulated precipitation over the Loess Plateau during 2000–2015. WRF simulation under the dynamic vegetation scenario (a), and under the static vegetation scenario (b). (c) The difference in trends between the dynamic and static vegetation scenarios.

than the cooling effect, and eventually caused the surface temperature to rise by 0.45°C and the near-surface temperature (2 m) to rise by 0.36°C . Vegetation restoration can also affect atmospheric water conditions, and the evapotranspiration increase resulted in a 3.25% increase in the water vapor content of the atmospheric boundary layer. In addition, the increases in surface temperature, near-surface temperature and sensible heat flux (3.79 W m^{-2}) also led to an increase in convective instability of the atmospheric boundary layer (convective available potential energy increased by +15.94%) and an increase in vertical velocity (+18.93%). Through the above physical process, large-scale vegetation restoration ultimately promoted an increase in regional precipitation.

5. Discussion

By considering the impact of vegetation dynamics on the

intensity of land-atmosphere interactions, this study coupled the dynamic changes of vegetation canopy parameters with the WRF-Noah model to construct a WRF-Noah land-atmosphere coupled model that takes into account the vegetation dynamic changes. Through comparing and analyzing the differences between the real scenario of vegetation restoration (WRF DYN) and the hypothetical scenario without vegetation restoration (WRF CTL), we found that considering the impact of vegetation dynamics can greatly improve the accuracy of the WRF-Noah model for regional precipitation simulation. The increases in evapotranspiration and water vapor flux, and changes in energy processes, caused by large-scale vegetation restoration have had a positive effect on the increase of local precipitation.

Vegetation restoration is a basic indicator of the improvement of regional ecological-environmental conditions. How to evaluate the effect of vegetation restoration, quantify the success of vegetation restoration, and modify the gov-

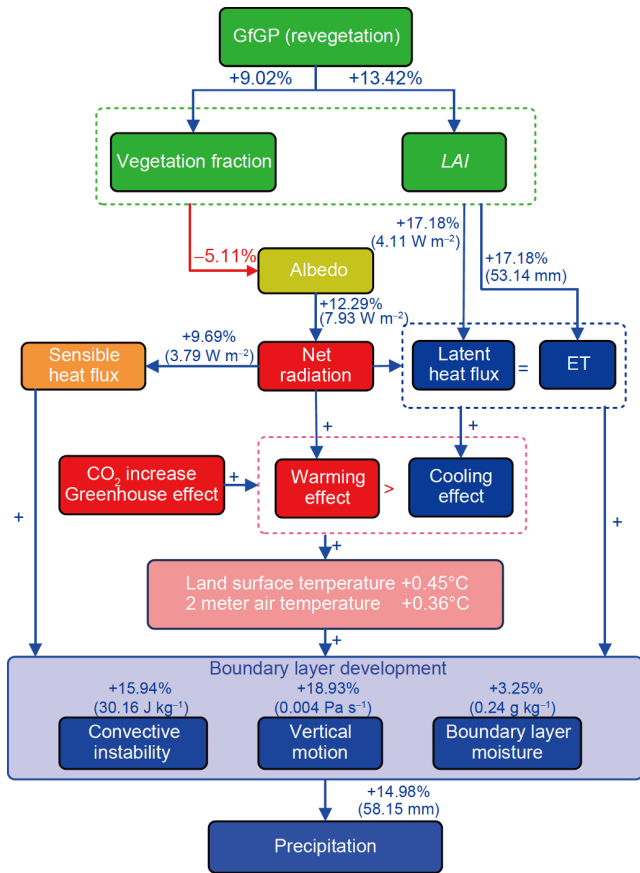


Figure 6 Schematic diagram of the mechanism responsible for the positive effect of GfGP on precipitation. The plus sign, “+”, denotes a positive contribution (green line), and the minus sign, “-”, denotes a negative contribution (red line). All the values in the diagram represent differences between the climatological values of the default scenario and dynamic scenario. Percentages are differences relative to the default scenario, also shown as the corresponding absolute values (in brackets).

ernance strategy in the future are of great significance to soil erosion management and vegetation restoration. The Loess Plateau is located in an arid to semi-arid area, where the amount of surface water is small and the groundwater is difficult to access because it is deeply buried. Therefore, rainwater resources have become the most important water source for vegetation restoration in this area (Wang et al., 2011). Large-scale vegetation restoration promotes an increase in local precipitation through feedbacks with regional climate. The increase in precipitation means an increase in the total amount of rainwater resources, and the temporal and spatial characteristics of rainwater resources determine the water use strategy of plants. Therefore, based on the balanced relationship of water consumption and replenishment, and through the efficient use of rainwater resources, proposing reasonable vegetation restoration strategies has become the basis for the management of ecological restoration and the efficient use of water resources across the Loess Plateau.

Large-scale vegetation restoration has changed the physi-

cal characteristics of the land surface, as well as the surface water balance and energy balance. Vegetation restoration can also increase the amount of water vapor transported to the atmosphere, by increasing evapotranspiration, thereby increasing regional atmospheric humidity and changing local precipitation and hydrological patterns. Therefore, when evaluating the rationality of vegetation restoration and proposing appropriate vegetation restoration strategies, it is necessary to consider the impact of large-scale vegetation restoration on the water cycle of the basin and on the intensity of land-atmosphere interactions. In addition, some areas did not follow the principle of sustainable use of water resources during the implementation of vegetation restoration. Poorly-managed and excessive vegetation restoration consumed a lot of water resources, breaking the original dynamic balance between the supply of rainwater resources and the water consumption of vegetation restoration, leading to the emergence of new ecological problems as represented by soil desiccation and vegetation degradation (Wang et al., 2010). Therefore, it is necessary to combine the WRF-Noah model with dynamic vegetation processes, and to quantitatively calculate the potential contribution of rainwater resources based on the effect of vegetation restoration on local precipitation. In addition, this work can help to actively develop and promote technological approaches to the efficient utilization of rainwater resources; it can identify the most suitable vegetation biomass that can be supported by rainwater resources in different regions, and on this basis, the results can be used to establish a vegetation restoration strategy based on the balance of water supply and demand on the Loess Plateau.

This study mainly discusses the effect of vegetation restoration on local precipitation across the Loess Plateau; however, when fully considering the feedbacks, it should be noted that changes in local precipitation also have an important impact on vegetation growth. Therefore, as models continue to develop, a full two-way coupling between the vegetation growth model and the regional climate model can be implemented in the future. In addition, further research should be carried out on the mutual feedback effects and interactions between climate change and vegetation dynamics, in order to provide further scientific support for the sustainable development of ecological restoration in the Loess Plateau.

6. Conclusion

This study analyzed the temporal and spatial trends of land use types, vegetation characteristics and surface parameters on the Loess Plateau from 2000 to 2015. By considering the impact of vegetation restoration on the hydrothermal cycle and the intensity of land-atmosphere interaction in the basin,

and by constructing a coupled land-atmosphere model that takes into account the vegetation dynamic changes, the effect of feedback between vegetation restoration and local precipitation was quantitatively evaluated. Since the implementation of large-scale vegetation restoration, the vegetation fraction and *LAI* of the Loess Plateau have increased by 40.7% and 18.3%, respectively, and the surface albedo has decreased by 7.5%. Vegetation fraction has been significantly improved. The hilly gully region of the south-east Loess Plateau has shown the most significant vegetation restoration effects, and large-scale vegetation restoration projects have achieved significant results. Vegetation restoration changes the underlying surface elements such as land use type, surface albedo, vegetation *LAI* and vegetation fraction, triggering a series of changes to net radiation, evapotranspiration, soil moisture, surface runoff, water vapor content of the atmospheric boundary layer, surface temperature, and sensible heat and latent heat fluxes. This results in a change in the intensity of the interaction between the land surface and the atmosphere, which has a feedback effect on the regional climate and local precipitation, and disrupts the original surface water balance.

In this study, two simulation experiments were set up to examine the real scenario with vegetation restoration and a hypothetical scenario without vegetation restoration. By comparing these two experiments, and analyzing the net impact of vegetation restoration on local precipitation, it was found that large-scale vegetation restoration has had a positive effect on local precipitation in the Loess Plateau. On the one hand, the increase in vegetation fraction leads to a decrease in regional albedo, which increases the amount of shortwave radiation received to heat the surface. On the other hand, increased vegetation leads to increased evapotranspiration and latent heat flux, which has a cooling effect on the ground. The heating effect is greater than the cooling effect, which eventually leads to an increase in the land surface temperature. Vegetation restoration can also affect atmospheric water conditions: the resulting increase in evapotranspiration increases the water vapor content in the atmospheric boundary layer by 3.25%. At the same time, the increases in surface temperature and sensible heat flux act to increase the convective instability and enhance vertical movement in the atmospheric boundary layer. Through these physical processes, large-scale vegetation restoration ultimately promoted the formation of local precipitation. Observational data show that precipitation on the Loess Plateau increased significantly (at a rate of 7.84 mm yr^{-2}) from 2000 to 2015. The simulation results show that large-scale vegetation restoration contributed about 37.4% of that precipitation increase in the study area, while water vapor from external circulation changes contributed the other 62.6%. The annual average precipitation in the vegetation restoration scenario on the Loess Plateau was 12.4% higher than

that of the scenario without vegetation restoration. The increase in precipitation means an increase in the available rainwater resources. In future, the development and application of technologies for efficient utilization of rainwater resources will help to alleviate the conflicts between water supply and demand caused by drought, water shortages and vegetation restoration.

Acknowledgements This work was supported by the National Key R&D Program of China (Grant No. 2020YFA0608403) and the National Natural Science Foundation of China (Grant Nos. 42022001, 41877150, 42041004 & 42001029).

References

- Bao J, Feng J, Wang Y. 2015. Dynamical downscaling simulation and future projection of precipitation over China. *J Geophys Res Atmos*, 120: 8227–8243
- Chen Y P, Wang K B, Lin Y S, Shi W Y, Song Y, He X H. 2015. Balancing green and grain trade. *Nat Geosci*, 8: 739–741
- Chen Y, Yang K, He J, Qin J, Shi J, Du J, He Q. 2011. Improving land surface temperature modeling for dry land of China. *J Geophys Res*, 116: D20104
- Chen F, Mitchell K, Schaake J, Xue Y, Pan H L, Koren V, Duan Q Y, Ek M, Betts A. 1996. Modeling of land surface evaporation by four schemes and comparison with FIFE observations. *J Geophys Res*, 101: 7251–7268
- Dudhia J. 1993. A nonhydrostatic version of the Penn State-NCAR mesoscale model: Validation tests and simulation of an Atlantic cyclone and cold front. *Mon Wea Rev*, 121: 1493–1513
- Emmanouil G, Vlachogiannis D, Sfetsos A. 2021. Exploring the ability of the WRF-ARW atmospheric model to simulate different meteorological conditions in Greece. *Atmos Res*, 247: 105226
- ESA. 2017. Land Cover CCI Product User Guide Version 2. Technical Report
- Feng X M, Fu B J, Piao S L, Wang S, Ciais P, Zeng Z Z, Lü Y H, Zeng Y, Li Y, Jiang X H, Wu B F. 2016. Revegetation in China's Loess Plateau is approaching sustainable water resource limits. *Nat Clim Change*, 6: 1019–1022
- Ganguly S, Friedl M A, Tan B, Zhang X Y, Verma M. 2010. Land surface phenology from MODIS: Characterization of the Collection 5 global land cover dynamics product. *Remote Sens Environ*, 114: 1805–1816
- Gao Y, Chen F, Miguez-Macho G, Li X. 2020. Understanding precipitation recycling over the Tibetan Plateau using tracer analysis with WRF. *Clim Dyn*, 55: 2921–2937
- Gibbard S, Caldeira K, Bala G, Phillips T J, Wickett M. 2005. Climate effects of global land cover change. *Geophys Res Lett*, 32: L23705
- He J, Yang K, Tang W, Lu H, Qin J, Chen Y, Li X. 2020. The first high-resolution meteorological forcing dataset for land process studies over China. *Sci Data*, 7: 1–11
- Hersbach H, Dee D. 2016. ERA5 reanalysis is in production. *ECMWF Newsletter*, 147: 5–6
- Hirsch A L, Pitman A J, Kala J. 2014. The role of land cover change in modulating the soil moisture-temperature land-atmosphere coupling strength over Australia. *Geophys Res Lett*, 41: 5883–5890
- Hu C H, Chen X J, Chen J G. 2008. Study on the spatial distribution of water and sediment in the Yellow River and its change process (in Chinese). *J Hydraul Eng*, 39: 518–527
- Hu Y, Zhang X Z, Mao R, Gong D Y, Liu H B, Yang J. 2015. Modeled responses of summer climate to realistic land use/cover changes from the 1980s to the 2000s over eastern China. *J Geophys Res Atmos*, 120: 167–179
- Jin J, Wen L. 2012. Evaluation of snowmelt simulation in the weather research and forecasting model. *J Geophys Res*, 117: D10110

- Kain J S. 2004. The Kain-Fritsch convective parameterization: An update. *J Appl Meteor*, 43: 170–181
- Liang W, Bai D, Wang F Y, Fu B J, Yan J P, Wang S, Yang Y T, Long D, Feng M Q. 2015. Quantifying the impacts of climate change and ecological restoration on streamflow changes based on a Budyko hydrological model in China's Loess Plateau. *Water Resour Res*, 51: 6500–6519
- Liu J Y, Shao Q Q, Yan X D, Fan W J, Deng X Zh, Zhan J Y, Gao X J, Huang L, Xu X L, Hu Y F, Wang J B, Kuang W H. 2011. Preliminary study on research progress and methods of land use change Impact on global climate (in Chinese). *Earth Sci Prog*, 26: 1015–1022
- Luo L H, Zhang Y N, Zhou J, Pan X D, Sun W J. 2013. Research on land surface process simulation of Qinghai-Tibet Plateau based on CLM model driven by WRF (in Chinese). *J Glaciol Geocryol*, 35: 553–564
- Mlawer E J, Taubman S J, Brown P D, Iacono M J, Clough S A. 1997. Radiative transfer for inhomogeneous atmospheres: RRTM, a validated correlated-k model for the longwave. *J Geophys Res*, 102: 16663–16682
- Nakanishi M, Niino H. 2006. An improved Mellor-Yamada level-3 model: Its numerical stability and application to a regional prediction of advection fog. *Bound-Layer Meteorol*, 119: 397–407
- Neale R, Hoskins B. 2010. Description of the NCAR community atmosphere model (CAM 5.0). NCAR Technical Note. Boulder: National Center for Atmospheric Research (NCAR)
- Piao S L, Zhang X P, Chen A P, Liu Q, Lian X, Wang X H, Peng S S, Wu X C. 2019. The impacts of climate extremes on the terrestrial carbon cycle: A review. *Sci China Earth Sci*, 62: 1551–1563
- Ren H C, Shi X L, Zhang Z Q. 2014. Analysis on the Characteristics of the Change of Leaf Area Index in China from 2003 to 2009 (in Chinese). *Meteorol Sci*, 34: 171–178
- Sen P K. 1968. Estimates of the regression coefficient Based on Kendall's Tau. *J Am Statist Associat*, 63: 1379–1389
- Su C H, Fu B J. 2013. Evolution of ecosystem services in the Chinese Loess Plateau under climatic and land use changes. *Glob Planet Change*, 101: 119–128
- Subin Z M, Riley W J, Jin J M, Christianson D S, Torn M S, Kueppers L M. 2011. Ecosystem feedbacks to climate change in California: Development, testing, and analysis using a coupled regional atmosphere and land surface model (WRF3-CLM3.5). *Earth Interact*, 15: 1–38
- Theil H. 1950. A rank-invariant method of linear and polynomial regression analysis. I, II, III. *Proc Roy Netherlands Acad Sci*, 53: 386–392, 521–525, 1397–1412
- Tang Q H. 2020. Global change hydrology: Terrestrial water cycle and global change (in Chinese). *Sci Sin Terr*, 50: 436–438
- Wang C H, Sun C. 2013. The establishment and preliminary test of a regional climate model (WRFC) based on WRF+CLM (in Chinese). *J Plateau Meteorol*, 32: 1626–1637
- Wang F, Wang Z M, Yang H B, Zhao Y. 2018. Study of the temporal and spatial patterns of drought in the Yellow River basin based on SPEI. *Sci China Earth Sci*, 61: 1098–1111
- Wang G Q, Zhang C C, Liu J H, Wei J H, Xue H, Li T J. 2006. Vegetation cover change and benefit analysis of water and sediment reduction in the sediment-rich and coarse sand regions of the Yellow River basin (in Chinese). *Sed Res*, 2: 10–16
- Wang S, Fu B J, Piao S L, Lü Y H, Ciais P, Feng X M, Wang Y F. 2016. Reduced sediment transport in the Yellow River due to anthropogenic changes. *Nat Geosci*, 9: 38–41
- Wang Y Q, Shao M A, Shao H B. 2010. A preliminary investigation of the dynamic characteristics of dried soil layers on the Loess Plateau of China. *J Hydrol*, 381: 9–17
- Wang Y Q, Shao M A, Zhu Y J, Liu Z P. 2011. Impacts of land use and plant characteristics on dried soil layers in different climatic regions on the Loess Plateau of China. *Agric For Meteorol*, 151: 437–448
- Wang Y Y, Xie Z H, Jia B H, Yu Y. 2015. Simulation and evaluation of China's regional vegetation total primary productivity based on the land surface process model CLM4 (in Chinese). *J Clim Environ Res*, 20: 97–110
- Wen X H, Lu S H, Jin J M. 2012. Integrating remote sensing data with WRF for improved simulations of Casis effects on local weather processes over an RRID region in northwestern China. *J Hydrometeorol*, 13: 573–587
- Wu L Y, Zhang J Y. 2013. Role of land-atmosphere coupling in summer droughts and floods over eastern China for the 1998 and 1999 cases. *Chin Sci Bull*, 58: 3978–3985
- Xiao Z Q, Liang S L, Wang J D, Yang X, Zhao X, Song J L. 2016. Long-Time-Series global land surface satellite leaf area index product derived from MODIS and AVHRR surface reflectance. *IEEE Trans Geosci Remote Sens*, 54: 5301–5318
- Xiao Z Q, Wang J D, Wang S. 2008. MODIS LAI products in China and their improvements (in Chinese). *J Remote Sens*, 12: 993–1000
- Xiong J S, Zhang Y, Wang S Y, Shang L Y, Chen Y G, Shen X Y. 2014. Effect of CLM4.0 soil moisture transmission scheme improvement in simulation of land surface process in Qinghai-Tibet Plateau (in Chinese). *J Plateau Meteorol*, 33: 323–336
- Yang D W, Zhang S L, Xu X Y. 2015. Analysis of the attribution of runoff changes in the Yellow River basin based on the water and heat coupled equilibrium equation (in Chinese). *Sci Sin Tech*, 45: 1024–1034
- Yang L, Zhang H D, Chen L D. 2018. Identification on threshold and efficiency of rainfall replenishment to soil water in semi-arid loess hilly areas. *Sci China Earth Sci*, 61: 292–301
- Yang F, Lu H, Yang K, He J, Wang W, Wright J S, Li C, Han M, Li Y. 2017. Evaluation of multiple forcing data sets for precipitation and shortwave radiation over major land areas of China. *Hydrol Earth Syst Sci*, 21: 5805–5821
- Yang K, He J, Tang W, Qin J, Cheng C C K. 2010. On downward shortwave and longwave radiations over high altitude regions: Observation and modeling in the Tibetan Plateau. *Agric For Meteorol*, 150: 38–46
- Yang Y, Zuo H C, Yang Q D, Du B, Wang X X, Wang M X, Wu J J. 2015. Numerical simulation research on the rapidly changing land surface process of the Desert-Steppe transition zone in arid regions by CLM4.0 model (in Chinese). *J Plateau Meteorol*, 34: 923–934
- Yu E T, Wang H J, Sun J Q. 2010. A quick report on a dynamical downscaling simulation over China using the nested model. *Atmos Ocean Sci Lett*, 3: 325–329
- Zhang B Q, He C S, Burnham M, Zhang L H. 2016. Evaluating the coupling effects of climate aridity and vegetation restoration on soil erosion over the Loess Plateau in China. *Sci Total Environ*, 539: 436–449
- Zhang B Q, Wu P T, Zhao X N. 2011. Monitoring and analysis of the spatiotemporal evolution of vegetation cover in the Loess Plateau in the past 30 years (in Chinese). *J Agric Eng*, 27: 287–293

(Responsible editor: Jianhui CHEN)